Contents lists available at ScienceDirect

Arabian Journal of Chemistry

journal homepage: www.ksu.edu.sa

Design of novel analogues of t-DPH1 with reduced cytotoxicity, taking the three conserved characteristics of the dermaseptin family as the feasible starting point

Haixin Qin [a,b,c], Weimin Zuo [a,b], Siyuan Luo [a,b], Lilin Ge [d], Lei Wang [c], Xiaoling Chen [c], Chengbang Ma [c], Hong-Ye Li [e], Tianbao Chen [c], Mei Zhou [c], Hang Fai Kwok [a,b,f,g,*]

[a] Institute of Translational Medicine, Faculty of Health Sciences, University of Macau, Avenida da Univer-sidade, Taipa, Macau
[b] Department of Biomedical Sciences, Faculty of Health Sciences, University of Macau, Avenida da Univer-sidade, Taipa, Macau
[c] School of Pharmacy, Queen's University Belfast, 97 Lisburn Road, Belfast BT9 7BL, UK
[d] College of Pharmacy, Nanjing University of Chinese Medicine, Nanjing 210023, China
[e] Key Laboratory of Eutrophication and Red Tide Prevention of Guangdong Higher Education Institutes, College of Life Science, Jinan University, Guangzhou 510632, China
[f] Cancer Centre, Faculty of Health Sciences, University of Macau, Avenida da Universidade, Taipa, Macau
[g] MoE Frontiers Science Center for Precision Oncology, University of Macau, Avenida da Universidade, Taipa, Macau

ARTICLE INFO

Keywords:
Antimicrobial peptide
Dermaseptin peptide
Peptide modification
Peptide cytotoxicity
Antibiotic and antiancer protoype drug
C. elegans

ABSTRACT

In recent years, there has been growing scientific interest in balancing the bioactivity and cytotoxicity of antimicrobial peptides (AMPs) for more comprehensive research and application. In this study, we focused on t-DPH1, a representative member of the dermaseptin family, as a template. We synthesized five analogues were synthesised to to assess the impact of three conserved features of the dermaseptin family (1. the tryptophan residue at 3rd position, 2. the consensus motif at mid-region, and 3. C-terminal amidation) on the bioactivity of t-DPH1 and their potential to reduce cytotoxicity. Our results demonstrated that analogues lacking an amino group at the C-terminus, specifically t-DPH1-NH_2, exhibited potent antimicrobial activity against Gram-negative bacteria, including *Escherichia coli* (*E. coli*) and *Klebsiella pneumoniae* (*K. pneumoniae*). Furthermore, t-DPH1-NH_2 retained its robust antiproliferative activity against the human non-small lung cancer cell line H157. Regarding cytotoxicity, t-DPH1-NH_2 displayed lower levels of haemolytic activity and cytotoxicity against two normal cell lines. Notably, we employed *C. elegans* as an *in vivo* model to assess the cytotoxicity of peptides, and the results revealed no induction of *in vivo* toxicity by t-DPH1-NH_2. Collectively, t-DPH1-NH_2 provides valuable insights for further investigation as promising bioactive peptide templates in the development of antibiotic and anticancer prototype drugs. The modifications implemented based on the conserved structure of the peptide family offer a new direction for reducing the cytotoxicity of peptides.

1. Introduction

In the last decade, extensive efforts have been dedicated to the discovery of novel antimicrobial and anticancer agents, driven by the escalating challenges of antibiotic and cancer drug resistance (Sharma et al., 2018; Munita and Arias, 2016; Norouzi et al., 2022; Chakraborty and Rahman, 2012). A pivotal milestone in antimicrobial research was reached in 1939 when Dubos derived an antimicrobial peptide (AMP) from a strain of soil bacillus, effectively protecting mice from pneumococcal infection (Van Epps, 2006). AMPs serve as the first line of defense in numerous organisms, playing a crucial role in preventing infections and exhibiting broad-spectrum antimicrobial activity against diverse bacteria, fungi and viruses (Jenssen et al., 2006). Apart from their remarkable bio-functional potential, the key advantage of AMPs in combating antibiotic resistance lies in their rapid killing kinetics, surpassing conventional antibiotics. This characteristic impedes bacteria from acquiring drug resistance in a timely manner (Mwangi et al., 2019). Consequently, AMPs are now recognized as an alternative to antibiotics

Peer review under responsibility of King Saud University.
* Corresponding author.
E-mail address: hfkwok@um.edu.mo (H.F. Kwok).

https://doi.org/10.1016/j.arabjc.2023.105420
Received 16 March 2023; Accepted 30 October 2023
Available online 31 October 2023

(Greber and Dawgul, 2017).

Amphibian skin stands out as an exceptional source of bioactive peptides among all origins of antimicrobial peptides (AMPs) (Vineeth Kumar and Sanil, 2017). These peptides, typically encoded genetically, exhibit remarkable similarity in their precursor signal sequences and intervening sequences (Nicolas and El Amri, 2009). Consequently, AMPs derived from amphibian skin can be categorized into superfamilies based on their conserved characteristics. One such superfamily is the dermaseptins, which are a diverse group of peptides produced by the skin secretions of tree frogs belonging to the genus *Phyllomedusa* (Mechlia et al., 2019). While dermaseptin display structural diversity, their biosynthetic precursor preproregions exhibit high conservation (Nicolas and El Amri, 2009). These cationic amphiphilic peptides consist of 24–34 amino acids and are characterized by an abundance of lysine (K) residues. The arrangement of amino acids forms two distinct lobes with negative and positive electrostatic surfaces, repsectively (Brand et al., 2006). In addition to their commonalities with AMPs from other superfamilies, dermaseptins possess three prominent conserved features, excluding the recently discovered Dermaseptin-S9: i) a conserved tryptophan (W) residue in the third position from the N- terminus; ii) the consensus motif 'AAXKAALXA' (with X representing any amino acid) in the mid-region; iii) the C-terminal amidation (Nicolas and El Amri, 2009; Mechlia et al., 2019; Thompson et al., 2007).

In both *in vitro* and *in vivo* studies, peptides from the dermaseptin family have demonstrated their utility in various antimicrobial applications. Notably, dermaseptins S1, S3, S4 and S5, derived from *Phyllomedusa. sauvagei*, exhibit potent and broad-spectrum antibacterial activity against a range of Gram-positive and multi-drug resistant Gram-negative bacteria (Xu and Lai, 2015; Zairi et al., 2009). Dermaseptin-H4, on the other hand, has been found to significantly inhibit the growth of Micrococcus. lysodeikticus, *Staphylococcus aureus* (*S. aureus*), *Escherichia coli* (*E. coli*) and *Pseudomonas aeruginosa* (*P. aeruginosa*), with minimum inhibitory concentration (MIC) values ranging from 0.4 to 0.8 μM (Thompson et al., 2007).

Moreover, owing to their positively charged and amphiphilic properties, dermaseptins have shown promising potential in interacting with negatively charged cancer cell membranes (Long et al., 2019; Ma et al., 2020). Previous studies on the structure–function relationship of dermaseptins have highlighted the role of the peptides' cationicity and amphiphilicity in membrane permeability, which is widely accepted as a fundamental mechanism of action for antimicrobial peptides (AMPs) (Lei et al., 2019). Initially, the cationic AMP molecules interact electrostatically with anionic phospholipids and acidic polymers on the cell membrane (Vineeth Kumar and Sanil, 2017). Subsequently, the hydrophobicity of AMPs enables their interaction with fatty acyl chains, leading to the formation of pores or alignment parallel to the cell membrane surface and ultimately disrupting the membrane integrity (Nguyen et al., 2011). However, it is important to note that the membrane-targeting mechanism of AMPs, while effective against microbial cells, can also pose a risk of attacking host cells, thus contributing to their cytotoxicity and hemolytic activity (Ongey et al., 2018). Therefore, the amphiphilic structure and positively charged groups of dermaseptin peptides play a pivotal role in their bioactivities as well as their potential cytotoxic effects.

Based on previous research, t-DPH1 has emerged as a newly discovered member of the dermaseptin family, exhibiting broad antimicrobial activities and potential antiproliferative effects on cancer cells (Qin et al., 2021). However, the considerable hemolytic activity and cytotoxicity towards normal cells, stemming from its mechanism of action involving cell membrane disruption, limit its further application. In this study, we aimed to address this limitation by designing a series of analogues of t-DPH1, wherein each of the three conserved characteristics of the dermaseptin family was systematically deleted or modified, with the goal of achieving a balance between bioactivity and cytotoxicity.

To evaluate the cytotoxicity of the designed analogues, we employed *Caenorhabditis elegans (C.elegans)* as a model organism. *C.elegans*, being a eukaryotic organism with well-established cell lineage, serves as a valuable tool for assessing the side effects and toxicity of drugs (Li et al., 2022; Lin et al., 2022). Compared to larger animal models such as mice or zebrafish, *C.elegans* possesses advantages such as its small size, short life cycle, and strong reproductive capability (David et al., 2003; Swain et al., 2004). Typically, the growth and movement of *C. elegans* are employed as indicators to reflect drug toxicity. Additionally, previous studies have demonstrated that exposure to polystyrene nanoparticles significantly reduces the head thrashes and body bends of both parent worms and their offspring in *C. elegans* (Zhang et al., 2022). Therefore, in this study, we assessed the toxicity of t-DPH1 and its analogues by monitoring the growth and movement of *C. elegans.*

2. Materials and methods

2.1. Peptide synthesis and purification

A Two-Channel Tribute Peptide Synthesiser (Protein Technologies, Tucson, AZ, USA) was used to synthesis the template peptide t-DPH1 and related modifiers based on the solid-phase peptide synthesis theory described before (Wu et al., 2018). Then, the lyophilized crude peptides were dissolved and injected into analytical reverse phase HPLC (Phenomenex Aeris PEPTIDE 5 μm XB-C18 column, 250 × 21.2 mm, Macclesfield, Cheshire, UK) for purification. The linear gradient was set from 100 % solution A (99.95/0.05(v/v) H_2O/TFA.) to 100 % solution B (0.05/19.95/80.00(v/v/v) TFA/H_2O/acetonitrile). Matrix-assisted laser dissociation ionized-time of flight mass spectrometry (MALDI-TOF MS) was used to detect the molecular masses of peptides. The analysis method was performed as in the previous study (Liu et al., 2022).

2.2. Physicochemical properties and secondary structure analysis

The sequences of analogues of t-DPH1 were put into the webserver, Heliquest (http://heliquest.ipmc.cnrs.fr/cgi-bin/ComputParamsV2.py), to determine their physicochemical properties and helical wheel plots were constructed to predict their secondary structures. To verify the secondary structures of synthesized peptides, a JASCO J815 Spectropolarimeter (JASCO Inc., Easton, MD, USA) was carried out for the circular dichroism (CD) analyses. The analytical method was performed as previously reported (Lu et al., 2022). T The peptide samples were dissolved in 50 % trifluoroethanol (TFE)/10 mM ammonium acetate buffer (NH4Ac) and 10 mM NH4Ac to reach a final concentration of 100 μM and then loaded into a 1-mm path length cuvette (Hellma Analytics, Essex, UK). CD spectra were measured at the range of 190–250 nm at 20 °C at 200 nm/min scanning speed with 1 nm bandwidth and 0.5 nm data pitch. Then the collected results were analyzed by the online analysis web server, K2D3 (https://cbdm-01.zdv.uni-mainz.de/~andrade/k2d3/).

2.3. Assessment of antimicrobial activity — Minimal inhibitory concentration (MIC) and minimal bactericidal concentration (MBC) assays

Seven different microbes were involved in this assay to evaluate the antimicrobial susceptibility of t-DPH1 and its analogues. The strains and numbers are listed in Table 1. All the bacteria were cultured in Mueller Hinton broth (MHB), and yeast was cultured in yeast extract peptone dextrose broth (YPD-B). For the experimental groups, microorganisms in log-phase (10^5 CFU/ml) were mixed with the peptides of the final concentration of 512 μM, 256 μM, 128 μM, 64 μM, 32 μM, 16 μM, 8 μM, 4 μM, 2 μM, 1 μM, in a 96-well plate. PBS was used as the negative control, norfloxacin and amphotericin B were used as the positive control for bacteria and yeast, respectively. This assay was repeated three times, and each time contained three replicates. As the previous study demonstrated, the MIC value represents the lowest concentration of

Table1
Seven microorganisms used in MIC and MBC assays.

	Microorganisms	Strain Number
Gram-positive bacteria	*S. aureus*	ATCC 6538
	Enterococcus faecalis (*E. faecalis*)	NCTC 12,697
	methicillin-resistant *Staphylococcus aureus* (MRSA)	NCTC 12,493
Gram-negative bacteria	*E. coli*	ATCC 8739
	P. aeruginosa	ATCC 9027
	K. pneumoniae	ATCC 43,816
Yeast	*Candida albicans* (*C. albicans*)	ATCC 10,231

peptides at which no visible growth of the microorganism after 24 h incubation (Ye et al., 2022). For the MBC assay, 10 μL of the medium from each clear well was inoculated onto a Mueller- Hinton agar (MHA) (for bacteria) or yeast extract peptone dextrose agar (YPD-A) (for yeast) plate and incubated for 24 h for measurement MBC values.

2.4. Assessment of mammalian cell proliferation inhibitory effect — MTT assays

The MTT assay was conducted to verify the proliferation inhibitory effect of t-DPH1 and its analogues. The related cell lines are listed in Table 2. The cell lines mentioned above were purchased from the American Type Culture Collection (ATCC, Manassas, VA, USA) and the European Collection of Cell Cultures (ECACC, Salisbury, UK) for this assay.

For the MTT assay, we referred to the previous research (Li et al., 2018). Eight thousand cells/per well were seeded in the 96 well plates overnight. For the peptide groups, the final concentration of peptides was from 100 μM to 10 nM. Negative control and positive control groups were spiked with the fresh serum-free medium containing equal amounts of PBS, and 0.1 %(w/v) Triton X-100, respectively. Then the 96-well plate was incubated at 37 °C with 5 % CO_2. After 24 h-incubation, ten microliters of MTT solution (5 mg/ml) (Sigma, UK) was added to each well and incubated in a dark environment for two hours. Then, the solution in each well was removed, and 100 μL of DMSO was added. Finally, the plate was shaken for 10 min on a shaking incubator before detecting the OD value using a Synergy HT plate reader (BioTek, USA) at $\lambda = 570$ nm. All the experimental groups required three replicates, and the experiment was repeated three times.

2.5. Haemolysis assay

Following the previous study, the haemolytic activity of t-DPH1 and its derivates were evaluated (Huang et al., 2017). The blood cells treated with 0.1 % Triton-X 100 were used as a positive control, and the blood cells treated with PBS were used as the negative control. After 2 h-incubation, the tube containing blood and different treatment were centrifuged and 100 μL supernatant from each sample were transferred to a new 96-well plate. The OD value of each well was measured with a Synergy HT plate reader (BioTek, Minneapolis, MN, USA) at an absorbance of 570 nm. The haemolysis effect (%) was calculated as below:

$$\text{Haemolysis}\,(\%) = \frac{\text{OD value(sample)} - \text{OD value(negative control)}}{\text{OD value(positive control)} - \text{OD value(negative control)}} \times 100\%$$

Table 2
Cell lines employed in MTT assays.

Cell lines		Strain Number
Human non-small cell lung cancer cell lines	NCI-H838	(ATCC® CRL-5844)
	NCI-H157	(ATCC® CRL-5802)
Human neuronal glioblastoma cancer cell line	U251MG	(ECACC 09063001)
Human prostate carcinoma cancer cell line	PC3	(ATCC® CRL-1435TM)
Human microvascular endothelial cell line	HMEC-1	(ATCC®-CRL-3243)
Human keratinocyte cell line	HaCaT	(ATCC®-PCS-200–011)

2.6. Assessment of the toxicity towards Caenorhabditis elegans

2.6.1. Culture and maintenance of Caenorhabditis elegans strains

Wide-type N2 *Caenorhabditis elegans* was obtained from Caenorhabditis Genetics Center (CGC, USA). The worms were maintained on the Nematode Growth Medium with a layer of Escherichia coli OP50 as food at 20 °C. The synchronized worms were obtained by putting pregnant worms on a nematode growth medium (NGM) plate to lay eggs for 2 h (Chen et al., 2021).

2.6.2. Assessment of body length and body width

L1 larva was collected by K medium (51 mM NaCl and 32 mM KCl). One hundred microliters of different concentrations of peptides (200 μM, 100 μM and 50 μM) were added to a 24-well plate. 0.5 % DMSO was applied as the control group. Then 50 μL of worms solutions was transferred into each well. Finally, concentrated OP50 solution (50 μL) was added as the food resource. The plate was placed at 20 °C for 72 h. Then the worms were anesthetized by NaN_3 (35 mM) and pictured by an EVOS M700 microscope (Thermo Fisher Scientific, UK). The body length and body width were measured by Image J software.

2.6.3. Determination of body bending and head swing

L1 worms were treated with different concentrations of drugs for 72 h. And 0.5 % DMSO was used as the control group. After treatment, the worms were transferred to a new NGM plate for 2 min recovery. Then the body bending and head swing was counted under an EVOS M700 microscope (Thermo Fisher Scientific, UK). Each index was measured for 15 s.

2.7. Statistical analysis

Statistical analysis was performed using GraphPad Prism software (Version 8.0, GraphPad Software Inc., San Diego, CA, USA). The p-values were calculated by a one-way or two-way ANOVA test from the mean values of the indicated data. Significant differences were demonstrated with asterisks (* $p < 0.05$; ** $p < 0.01$; *** $p < 0.001$, **** $p < 0.0001$).

3. Results

3.1. Peptide design

The sequence of t-DPH1 (parent peptide) and its five analogues are listed in Table 3. There were three modification ideas related to the conserved characteristics of Dermaseptin family: (1) the removal of the tryptophan (W) residue at the 3rd position; (2) the modification of the C-terminus; (3) the truncation of the consensus motif.

For the first idea, the hydrophobic W^3 residue of the t-DPH1 was removed, and the modified analogue was named, t-DPH1-W. This modification aimed to observe the effect of eliminating the conserved W^3 residue in the sequence of dermaseptin peptides on the bioactivity of the peptide.

There were two products from the modification idea of C-terminal modification. Firstly, based on the result of molecular cloning, the amide group ($–NH_2$) located at the C-terminus was removed, and the 'GEQ' residues removed in the post-translational modification process were added back to the C-terminus of the peptide sequence to obtain the natural-occurring peptide without C-terminal amidation, DPH1.

Table 3
Primary structures and physiochemical properties of t-DPH1 and its analogues.

Peptide	Amino acid sequence	Length (aa)	Net charge	Hydrophobicity <H>	Hydrophobic moment < μH>	% of α-helicity in 50 % TFE
t-DPH1	GLWSKIKNVAAAAGKAALGAL-NH_2	21	+4	0.425	0.337	53.64
t-DPH1-W	GL-SKIKNVAAAAGKAALGAL-NH_2	20	+4	0.334	0.336	52.88
DPH1	GLWSKIKNVAAAAGKAALGALGEQ	24	+2	0.336	0.335	55.78
t-DPH1-NH_2	GLWSKIKNVAAAAGKAALGAL	21	+3	0.425	0.337	53.75
t-DPH1a	GLWSKIKNVAAAAGKAAL-NH_2	18	+4	0.384	0.363	49.15
t-DPH1b	GLWSKIKNVAAA-NH_2	12	+3	0.430	0.455	39.16

Secondly, the amide group located at the C-terminus was removed directly to obtain the other analogue, t-DPH1-NH_2. The design of DPH1 and t-DPH1-NH_2 aimed to observe the effect of C-terminal amidation on the bioactivities of the peptide.

The last modification idea was to truncate the parent peptide from the consensus motif. (AXKAALXA, where X can be any amino acid). t-DPH1a and t-DPH1b were the C-terminally truncated products based on t-DPH1. t-DPH1a was obtained by removing three residues 'GAL' at the C-terminus of t-DPH1, with a sequence of 18 amino acids. Then, t-DPH1a was further truncated by removing six residues "AGKAAL" at the C-terminus to obtain t-DPH1b, composed of 12 amino acid residues and without the consensus motif of the dermaseptin family. The design of t-DPH1a and t-DPH1b aimed to observe the effect of the consensus motif (AGKAALGA) on the bioactivities of t-DPH1.

The hash (-) in the sequence indicates the removed amino acid. Amino acids that differ from the parent peptide, t-DPH1 (Qin et al., 2021), are highlighted in red. The conserved sequences of the dermaseptin family are single-underlined.

3.2. Purification and identification of t-DPH1's analogues

After synthesis, analogues of t-DPH1, were purified by reverse phase HPLC (Supplementary Materials Figure S1). The mass spectra of the collected samples containing the pure peptides (Supplementary Materials Figure S2), where there was only one major peak along with the sodium or potassium adduct following that peak in each chromatogram, confirmed the molecular masses of the purified peptides.

3.3. Secondary structures and physicochemical properties of t-DPH1's analogues

As reported, dermaseptin peptides can form amphiphilic α-helical structures in non-polar solvents and cell membrane environments (Conceicao et al., 2006). The online analysis tool, Heliquest (https://he

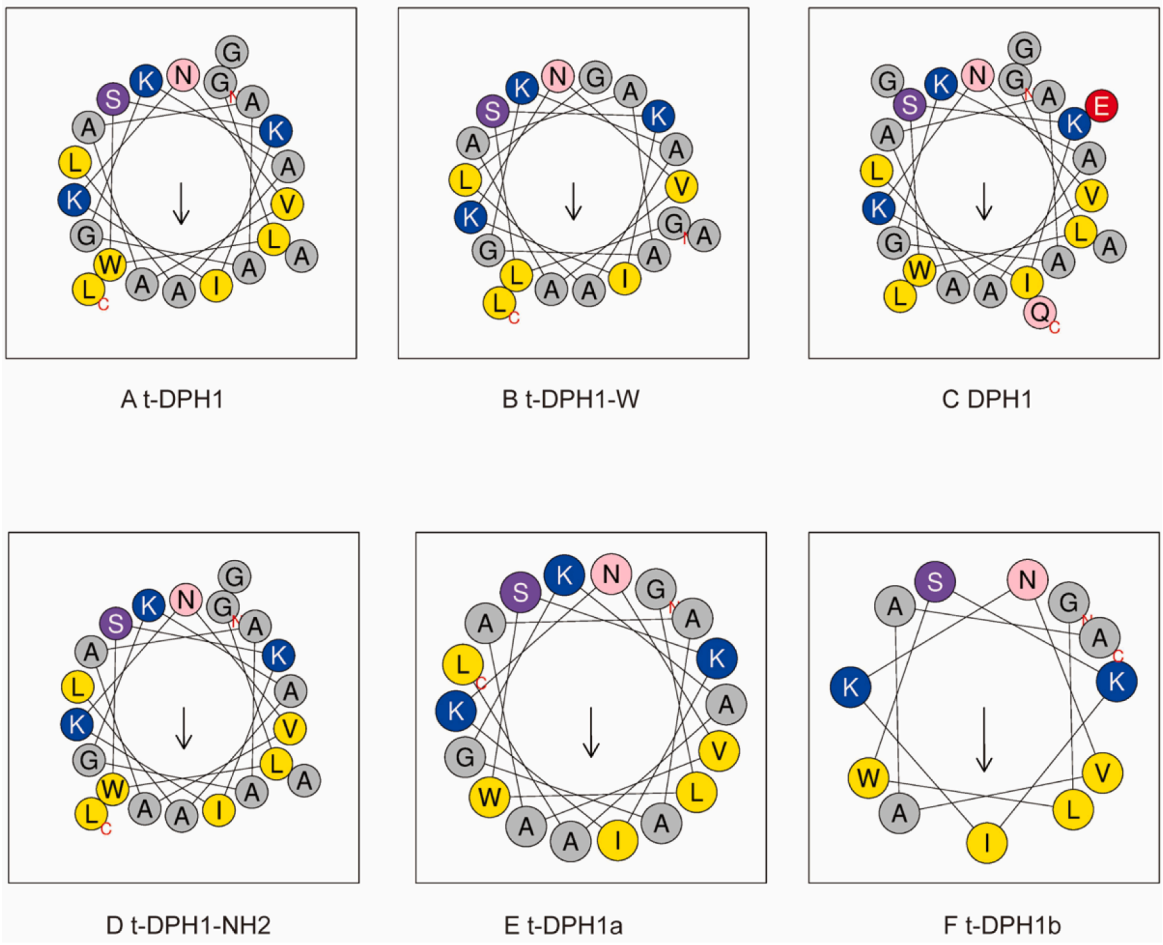

Fig. 1. Helical wheel plots (A to F) of t-DPH1 and its analogues. The arrow in each picture points to the hydrophobic face of the peptide. Amino acids with different properties are presented in different colors. (grey: non-polar residue; blue: positively charged residue; red: negatively charged residue; yellow: hydrophobic residue, pink: asparagine and glutamine, purple: serine).

liquest.ipmc.cnrs.fr/cgi-bin/ComputParams.py), was used to predict the secondary structures of analogues of t-DPH1. As shown in Fig. 1, t-DPH1 and t-DPH1-NH_2 had the same hydrophobic face (AVLAAIAAWL). Except for these, DPH1 and t-DPH1a had incomplete hydrophobic faces (DPH1: AIAA; t-DPH1a: AVLAIAAW). Due to the deletion of the W^3 residue, t-DPH1-W possessed a different hydrophobic face (AVGAAIAA). The last designed analogue, t-DPH1b did not possess a hydrophobic face.

The physicochemical properties of designed analogues are listed in Table 3, and the properties of the parent peptide t-DPH1 are also listed for comparison (Qin et al., 2021). After adding the "GEQ" to the C-terminus, the net charge of DPH1 was reduced to + 2; t-DPH1-W and t-DPH1a kept the same net charge as t-DPH1. After removing the whole consensus motif, the net charge of t-DPH1b was reduced to + 3 but achieved a higher hydrophobicity and hydrophobic moment (0.430 and 0.455). Except for t-DPH1b, all the designed analogues displayed similar amphipathy (with hydrophobic moments from 0.33 to 0.36). Since the –NH_2 group at the C-terminus does not participate in the formation of the α-helix, t-DPH1-NH_2 had the same hydrophobicity and hydrophobic moment as the parent peptide. Still, the net charge of t-DPH1-NH_2 was one less than that of t-DPH1.

The secondary conformations of t-DPH1 and its analogues were tested by CD analysis. All tested peptides displayed random coils in an aqueous solution (10 mM NH_4Ac) but tended to fold into helical structures in a membrane-mimetic environment (50 % TFE in 10 mM NH_4Ac solution) (Fig. 2). The data were submitted to the K2D3 webserver to analyze the α-helicity (%) of each peptide. Except for two C-terminal truncated peptides, t-DPH1a and t-DPH1b, parent peptides and modified peptides showed similar α-helical content in membrane-mimetic conditions (from 52.88 % to 55.78 %). However, due to the removal of the consensus motif, t-DPH1b possessed the lowest α-helicity (39.16 %).

3.4. Antimicrobial activity of t-DPH1 and analogues

The values for the MICs and MBCs of t-DPH1 and analogues against different microorganisms are listed in Table 4. Consistent with the previous study (Qin et al., 2021), the parent peptide t-DPH1 showed broad-spectrum antimicrobial activity against all seven microorganisms.

The analogues of t-DPH1 showed various potencies in killing the tested microorganisms. After removing the C-terminal amidation, the antimicrobial activity of t-DPH1-NH_2 against Gram-positive bacteria decreased significantly, and the MICs of t-DPH1-NH_2 against *S. aureus* and *MRSA* were 8-fold higher than that of t-DPH1. DPH1 and the natural peptide with 'GEQ' at the C-terminus were nearly devoid of antimicrobial activity. It could only kill *S. aureus* and *C. albicans* at high concentrations (MIC/MBC: 256 μM/256 μM). The removal of W^3 residue also resulted in decreased antimicrobial activity. t-DPH1-W could only kill *E. coli* and *C. albicans* at high concentrations (MICs: 128 μM and 256 μM, respectively). t-DPH1a, with deletion of the three residues 'GAL' at the C-terminus of t-DPH1 and part of the consensus motif (AGKAAL) of the dermaseptin family, retained certain antimicrobial activities. However, compared with the parent peptide, the MIC values against three tested Gram-positive bacteria were twice as high as those of t-DPH1. The

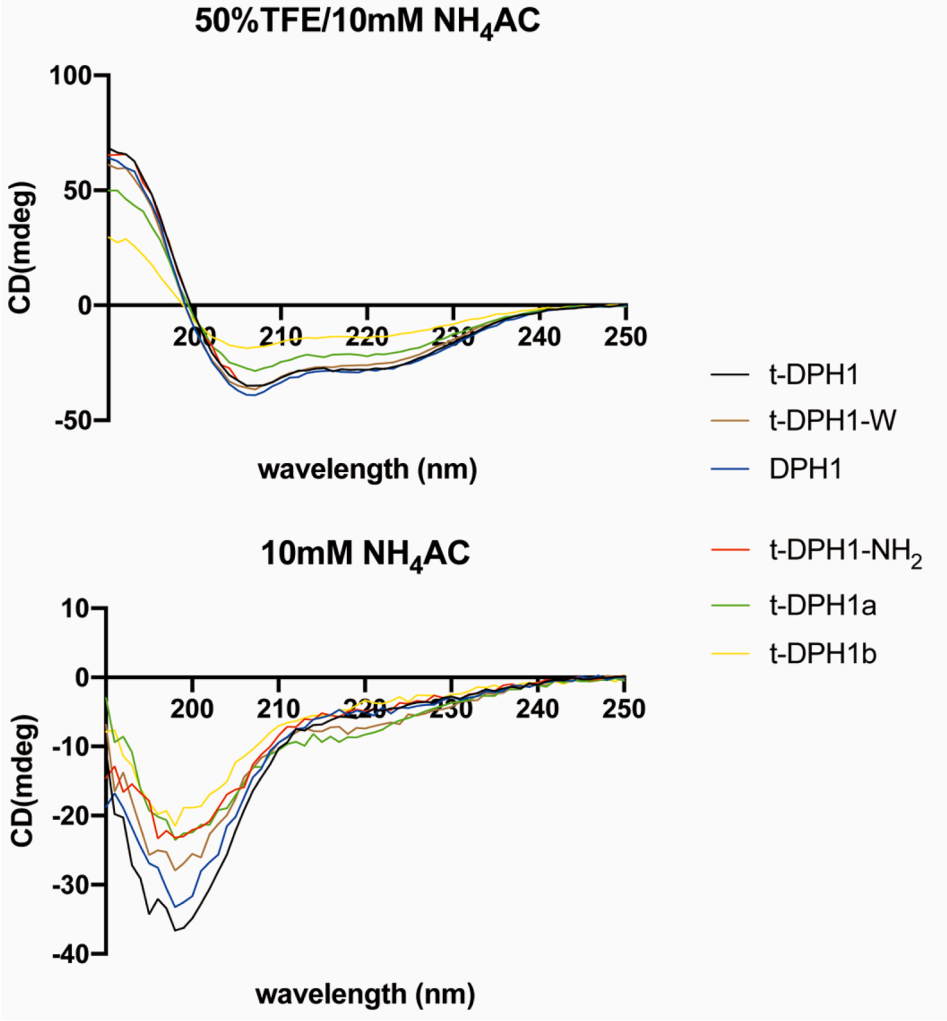

Fig. 2. Circular dichroism spectra of t-DPH1 and its analogues (100 μM) in 50 % TFE/NH_4AC and 10 mM NH_4AC buffer.

Table 4
MICs/MBCs (μM) of t-DPH1 and its analogues.

	t-DPH1	t-DPH1-NH_2	DPH1	t-DPH1-W	t-DPH1a	t-DPH1b
S. aureus (ATCC 6538)	8/16	64/128	256/256	>512/>512	16/32	512/512
MRSA (NCTC 12493)	16/32	128/256	>512/>512	>512/>512	32/64	512/>512
E. faecalis (NCTC 12697)	128/256	128/256	>512/>512	>512/>512	256/256	>512/>512
E. coli (ATCC 8739)	4/8	4/8	>512/>512	128/256	8/16	512/>512
K. pneumoniae (ATCC 43816)	8/16	16/32	>512/>512	512/>512	>512/>512	512/>512
P. aeruginosa (ATCC 9027)	16/32	64/128	>512/>512	>512/>512	256/512	>512/>512
C. albicans (ATCC 10231)	64/128	128/256	256/256	256/512	64/128	512/512

designed analogue without the consensus motif of the dermaseptin family, t-DPH1b, lost all antimicrobial potency.

3.5. Antiproliferative activity of t-DPH1 and its analogues

As reported before (Qin et al., 2021), synthetic peptide t-DPH1 displayed a broad-spectrum antiproliferative effect against PC-3, H838, H157 and U251MG cancer cells (Table 5).

After removing the C-terminal amidation, the antiproliferative activities of DPH1 and t-DPH1-NH_2 against PC-3, H157 and U251MG cell lines decreased compared to that of t-DPH1. Still, they nearly maintained the same abilities when inhibiting the growth of the H838 cell line.

The removal of the W^3 residue resulted in an obvious decrease in the antiproliferative activity of t-DPH1-W. Even at a high concentration (100 μM), the cell viability of all tested cell lines was higher than 60 % (Fig. 3).

When the consensus motif was partly removed, t-DPH1a maintained the inhibitory effect against the H157 cell line, with an IC_{50} value of 18.98 μM. Except for this, the antiproliferative effects of t-DPH1a against tested cell lines were not revealed when treated with 10 μM of peptide; the cell viabilities of those cell lines were higher than 80 %. When the consensus motif was removed, t-DPH1b almost totally lost its antiproliferative activity.

'NS' means that compared with the negative control group, peptides had no significant difference in inhibiting the growth of tested cell lines at tested concentrations (data not shown).

3.6. Cytotoxicity of t-DPH1 and its analogues

3.6.1. Haemolytic activity

As shown in Fig. 4, except for parent peptide t-DPH1, all the other designed analogues were found to generate low levels of haemolysis (less than 10 %) at the tested concentrations. However, at a high concentration (10^{-4} M), t-DPH1 showed significant haemolytic activity (around 50 %) (Qin et al., 2021). Furthermore, compared with parent peptide t-DPH1, all the designed analogues achieved higher HC_{50} values (Table 6). Among these, t-DPH1-W displayed the lowest haemolytic activity, with the HC_{50} value of 5563 μM.

Table 5
Antiproliferative activities [IC_{50} (μM)] of t-DPH1 and its analogues against tested cell lines.

	PC-3	H838	H157	U251MG
t-DPH1	14.67	23.51	10.20	34.25
DPH1	48.46	27.02	17.70	NS
t-DPH1-NH_2	29.22	23.56	21.76	NS
t-DPH1-W	223.6	269.2	135.5	97.82
t-DPH1a	97.99	125.2	18.98	NS
t-DPH1b	273.2	307.8	557.7	225.5

3.6.2. Antiproliferative activity against HMEC-1 and HaCaT

As shown in Fig. 5, parent peptide t-DPH1 showed inhibitory effects on the proliferation of normal human cell lines HMEC-1 and HaCaT at a high concentration (100 μM). All the designed analogues displayed weaker inhibitory effects towards two tested human normal cell lines. The cell viabilities of HMEC-1 were over 70 % even when treated with a high concentration of peptides.

Apart from DPH1 and t-DPH1a, the other three designed analogues did not show antiproliferative effects against HaCaT cell line. The IC50 values of t-DPH1a and t-DPH1 against HaCaT cell line were almost identical (IC50s: 174.1 and 175.6 μM, respectively) (Table 7).

3.6.3. In vivo toxicity of t-DPH1 and its analogues

The in-vivo toxicity of t-DPH1 and its analogues was evaluated by measuring the growth (body length and body width) and locomotion behavior (head thrashes and body bending) of *C. elegans* (Fig. 6). When treated with high concentrations (200 and 100 μM) of t-DPH1, the two indexes of *C. elegans* growth decreased significantly compared with the negative control group (Table 8). Apart from t-DPH1, all the designed analogues showed pretty low toxicity in the growth of *C. elegans*. Also, as shown in Table 9, all the peptides did not influence the movement of *C. elegans* in 15 s.

4. Discussion

AMPs have garnered significant attention as potential alternative antimicrobial agents due to their role in immune defense (Daum et al., 2012). Among these, the dermaseptins have emerged as a superfamily of peptides that have been extensively studied and demonstrated to possess broad-spectrum antimicrobial activity (Amiche and Galanth, 2011). While dermaseptins exhibit structural and functional diversity, they shared three conserved characteristics, namely the presence of a tryptophan residue at the 3rd position, the motif AAXKAALXA in the mid-region, and C-terminal amidation. These conserved features reflects their evolutionary relationships (Nicolas and El Amri, 2009).

The novel peptide t-DPH1, which was first reported in 2021, belongs to the dermaseptin superfamily and exhibits characteristics typical of this family, including the presence of three conserved features mentioned earlier (Qin et al., 2021). t-DPH1 has demonstrated dual effects against seven tested microorganisms and four tested human cancer cell lines (Qin et al., 2021). However, it is noteworthy that t-DPH1 also exhibited high levels of haemolytic activity and cytotoxicity towards normal human cell lines. The bioactivity of dermaseptin peptides is closely linked to their membrane destruction mechanism and cytotoxicity (Abed et al., 2013). To address these limitations, we focused on the three conserved characteristics of dermaseptins as a starting point for designing a series of analogues. The aim was to achieve a balance between the bioactivities of t-DPH1 and explore the structure–activity relationships within the dermaseptin family.

Similar to other dermaseptins (Bartels et al., 2019), the highly conserved tryptophan residue is located at the 3rd position from the N-terminus of t-DPH1. Analysis using Heliquest, a tool for predicting helical structures, revealed that the Trp^3 residue contributes to the formation of the hydrophobic face of t-DPH1. Deletion of the conserved Trp^3 residue in the modified peptide, t-DPH1-W, did not significantly alter its amphiphilicity and α-helicity proportions compared to the parent peptide. However, the hydrophobicity of t-DPH1-W decreased significantly. As a result, t-DPH1-W nearly lost its antimicrobial activity and only exhibited inhibitory effects on *E. coli* at high concentrations (MIC/MBC: 128 μM/256 μM). Similarly, the antiproliferative effect of t-DPH1-W on the four-tested cancer cell lines was significantly reduced

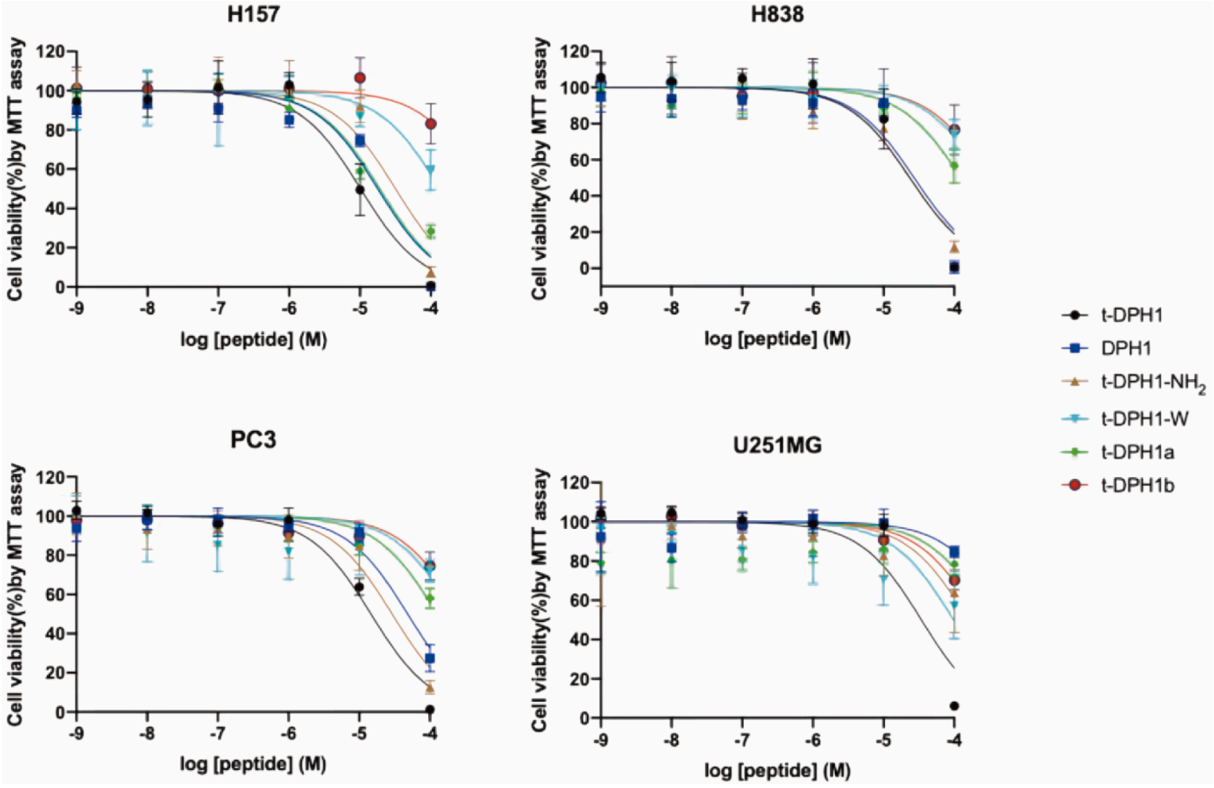

Fig. 3. The effects of t-DPH1 and its analogues on the proliferation of four cancer cell lines. The error bar indicated the *SEM* of nine replications.

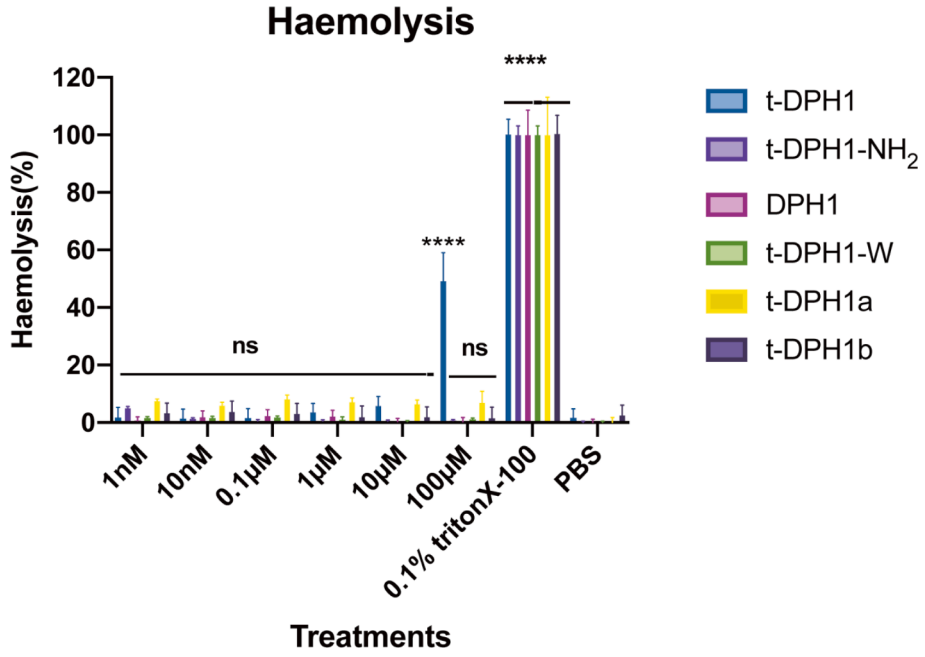

Fig. 4. Haemolytic activities of t-DPH1 and its analogues. The 0.1 % Triton-X 100 group was the positive control, and the PBS group was the negative control. Two-way ANOVA analyzed the data by comparing the haemolysis rate of different peptides in a series of concentrations with the negative control group. The significance is demonstrated with asterisks (* $p < 0.05$; ** $p < 0.01$; *** $p < 0.001$; **** $p < 0.0001$), and ns means there is no significant difference between peptide treatment groups and the negative control group. The error bar indicates the *SEM* of nine replicates.

compared to that of t-DPH1. These findings highlight the essential role of the Trp3 residue in the bioactivities of t-DPH1.

Hydrophobicity plays a crucial role in the bioactivities of AMPs, as supported by previous studies (Brogden, 2005; Huang et al., 2010). During the conformational transition of AMPs in the membrane environment, the hydrophobic regions of their α-helical structures interact with the complementary hydrophobic components of the cell membrane, facilitating their insertion into the membrane (Lee et al., 2002). Additionally, the Trp residue, especially when located near the N-terminus, has been shown to serve as an anchor in the membrane

Table 6
HC_{50} values of t-DPH1 and its analogues.

Peptides	HC_{50} (μM)
t-DPH1	106.4
t-DPH1-NH_2	1839
DPH1	3377
t-DPH1-W	5563
t-DPH1a	1119
t-DPH1-b	2567

disruption effect of AMPs (He et al., 2020; Arias et al., 2014). This is attributed to the aromatic side chain of tryptophan (the indole ring), which enables the peptide to penetrate deeper into the hydrophobic membrane environment. Consequently, the peptide can reside in the complex interface environment and interact effectively with the membrane (Yau et al., 1998; Hu et al., 1993). In the case of t-DPH1, the deletion of Trp^3 resulted in a significant weakening of its bioactivities, thus confirming the universality of the aforementioned theories.

The consensus motif (AXKAALXA) at the C-terminus is another characteristic of the dermaseptin family, and its effect in t-DPH1 was investigated through C-terminal truncation experiments. Analysis of helical wheel plots revealed that the four alanine residues within the consensus sequence contribute to the formation of the hydrophobic face of t-DPH1, resulting in strong hydrophobicity of the parent peptide. Partial deletion of two amino acids (Gly19 and Ala20) in the conserved sequence led to an incomplete hydrophobic face in t-DPH1a, while complete deletion of the entire consensus sequence in t-DPH1b prevented the formation of a hydrophobic face. Consequently, the circular

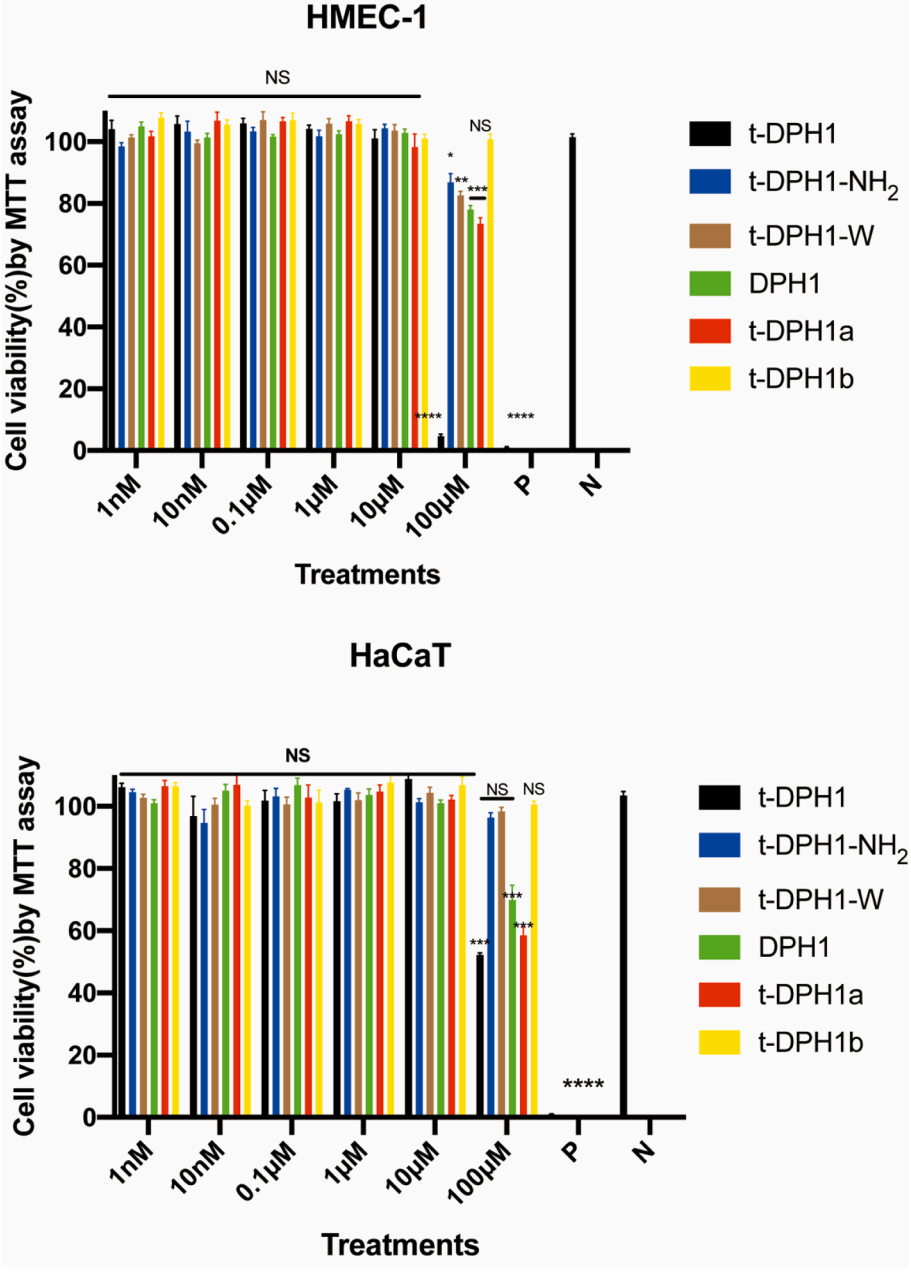

Fig. 5. The cytotoxicity of t-DPH1 and its designed derivatives on HMEC-1(top) and HaCaT (bottom). 'P' represents the positive control group (0.1 % Triton-X 100), and 'N' represents the negative control group (PBS). Two-way ANOVA analyzed the data by comparing the haemolysis rate of different peptides in a series of concentrations with the negative control group. The significance is demonstrated with asterisks (* $p < 0.05$; ** $p < 0.01$; *** $p < 0.001$; **** $p < 0.0001$), and NS means there is no significant difference between peptide treatment groups and the negative control group. The error bar indicates the *SEM* of nine replicates.

Table 7
IC_{50}s of t-DPH1 and its analogues against HMEC-1 and HaCaT (μM).

	t-DPH1	t-DPH1-NH_2	t-DPH1-W	DPH1	t-DPH1a	t-DPH1b
HMEC-1	29.85	650.2	487.9	449.4	241.4	NS
HaCaT	175.6	NS	NS	217.5	174.1	NS

'NS' means no significant difference between peptide treatment groups and the negative control group.

dichroism results analyzed using K2D3 demonstrated a significant decrease in the α-helicity proportion of t-DPH1a and t-DPH1b compared to the parent peptide. However, it is important to note that upon reaching the membrane environment through electrostatic interactions, the conformational transformation of AMPs into α-helical structures is crucial for their interaction with the membrane (Huang et al., 2010). The transformed α-helix structure exhibits amphiphilicity, causing the hydrophobic residues to face the hydrophobic core of the membrane. This process leads to the disruption of bilayer curvature and eventual micellar decomposition of the membrane (Oren and Shai, 1998). The antimicrobial evaluation of t-DPH1a and t-DPH1b supported these theories, as the MICs/MBCs against the tested microorganisms for t-DPH1a increased two-fold or more compared to t-DPH1, and t-DPH1b nearly lost all of its bioactivities.

As previous studies have shown, dermaseptins typically end with a -Glycine(G)-Glutamine(E)-Glutamic acid(Q) motif at the C-terminus and

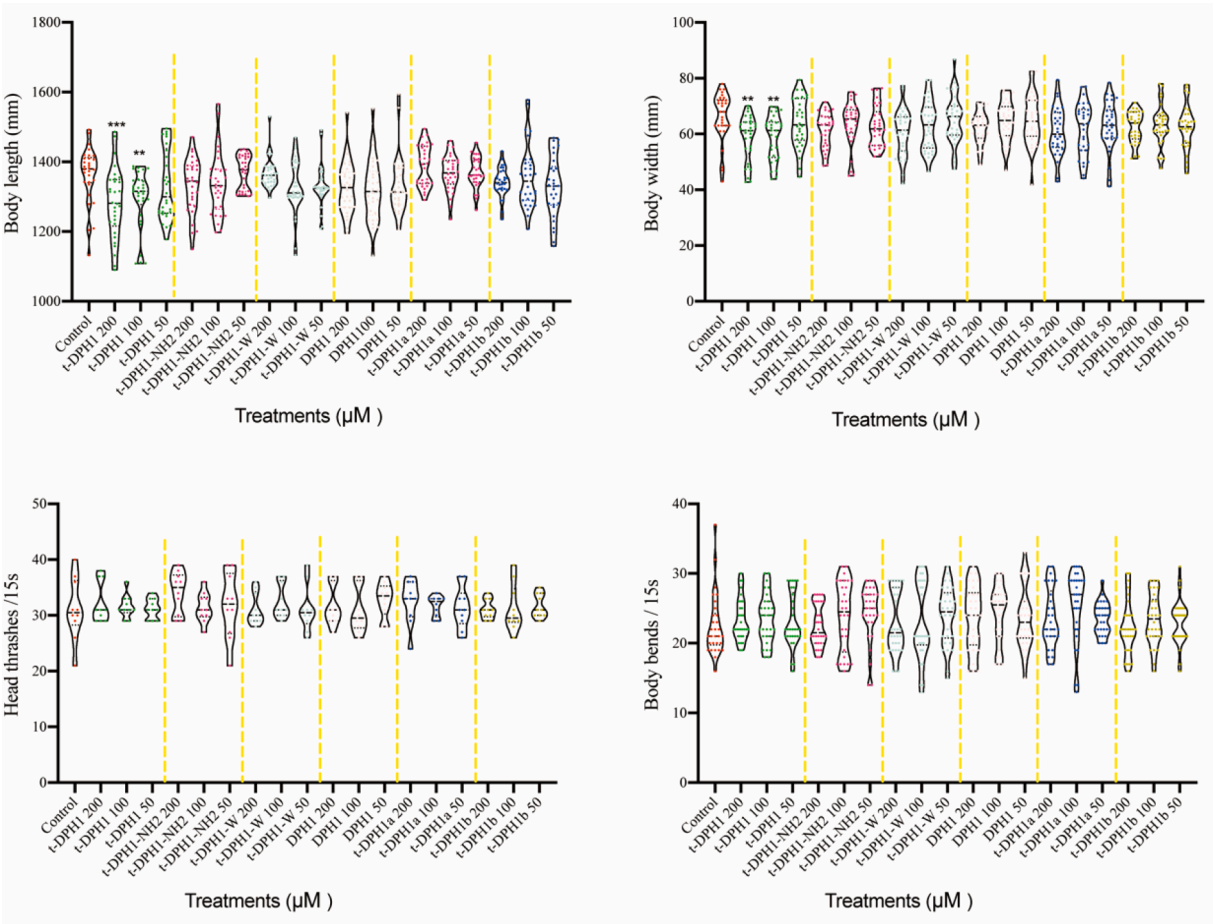

Fig. 6. The effect of t-DPH1 and its analogues on the growth (body length and body width) and locomotion behavior (head thrashes and body bends) of *C. elegans*. *** compared with negative control group, $p < 0.001$; ** compared with negative control group, $p < 0.01$.

Table 8
The mean body length and body width of worms with different peptide treatments.

	Body length (mm) Peptide concentration (μM)			Body width (mm)		
	200	100	50	200	100	50
t-DPH1	1281.85 ± 100.38***	1294.192 ± 83.28**	1332.65 ± 100.77	58.64 ± 8.12**	58.73 ± 7.92**	63.92 ± 8.83
t-DPH1-NH_2	1332.16 ± 77.90	1338.06 ± 91.12	1369.83 ± 49.10	61.26 ± 6.41	63.55 ± 8.07	62.67 ± 7.35
t-DPH1-W	1366.71 ± 44.00	1328.18 ± 78.12	1329.82 ± 59.31	60.77 ± 8.39	62.90 ± 8.78	65.29 ± 8.80
DPH1	1326.17 ± 74.50	1318.90 ± 88.77	1331.17 ± 84.72	62.23 ± 5.78	64.50 ± 7.30	64.90 ± 8.98
t-DPH1a	1388.83 ± 58.85	1366.96 ± 52.09	1368.89 ± 44.32	60.88 ± 8.63	61.70 ± 9.43	62.81 ± 8.81
t-DPH1b	1341.84 ± 41.80	1356.78 ± 90.96	1327.30 ± 87.15	63.37 ± 5.64	63.26 ± 7.34	62.51 ± 8.01
NC	1364.35 ± 74.50			66.09 ± 8.82		

'NC' means negative control group. *** compared with negative control group, $p < 0.001$; ** compared with negative control group, $p < 0.01$. The data was shown as mean ± standard division.

Table 9
The locomotion behavior of worms with different peptide treatments.

	Head thrashes/15 s Peptide concentration (μM)			Body bending/15 s		
	200	100	50	200	100	50
t-DPH1	32.2 ± 3.6	31.6 ± 2.1	31.2 ± 1.8	23.4 ± 3.1	23.5 ± 3.5	23.1 ± 3.9
t-DPH1-NH_2	34.1 ± 3.7	31.4 ± 2.6	31.7 ± 5.9	22.6 ± 3.0	23.9 ± 4.9	24.4 ± 4.0
t-DPH1-W	31.1 ± 2.8	32.5 ± 3.1	31.1 ± 4.0	22.8 ± 4.5	23.1 ± 5.6	23.9 ± 4.1
DPH1	31.8 ± 3.6	31.0 ± 4.2	32.8 ± 3.1	23.7 ± 4.6	24.3 ± 4.2	23.5 ± 4.4
t-DPH1a	32.5 ± 3.9	31.7 ± 1.8	31.4 ± 3.7	23.5 ± 4.3	25.3 ± 5.2	23.5 ± 2.3
t-DPH1b	31.1 ± 1.7	31.2 ± 4.2	31.7 ± 2.1	22.2 ± 3.9	23.4 ± 3.6	23.1 ± 3.2
NC	31.1 ± 5.5			22.5 ± 4.4		

'NC' means negative control group. The data was shown as mean ± standard division.

undergo post-translational modification to synthesize mature peptides (Thompson et al., 2007). During this process, carboxypeptidase cleaves the peptide bond between Gly and Glu, resulting in the removal of Glu and Gln. Gly serves as the amide donor in a two-step α-amidating reaction (Bradbury et al., 1982). The sequence of t-DPH1, which ends with an amino group, aligns with this regularity. Our results indicate that the naturally occurring peptide without post-translational modification, DPH1, exhibits weak antimicrobial potency. However, when we retained the post-translational modification process but only deleted the amide group at the C-terminus, the designed analogue t-DPH1-NH_2 maintained antimicrobial activity against gram-negative bacteria while significantly reducing its haemolytic activity. This suggests that the post-translational modification process is necessary to achieve the antimicrobial activity of t-DPH1, but C-terminal amidation is not crucial. This phenomenon may be explained by the reduced cationic property of the modified peptides. The positively charged amide group provides an additional net charge to the peptide, keeping the net charge of t-DPH1 within a reasonable range (+3 to + 10) (Torres et al., 2019). However, when the -GEQ residues replace the amide group, the net charge of DPH1 is reduced to + 2, weakening its interaction with the cell membrane (Liang et al., 2019).

Interestingly, it is worth noting that both DPH1 and t-DPH1-NH_2 still retain the ability to inhibit the growth of the human non-small lung cancer cell line, H157. Compared to t-DPH1, these analogues demonstrate lower cytotoxicity to the human normal cell line HMEC and exhibit low haemolytic activity even at high concentrations (100 μM). When evaluating the toxicity of these peptides *in vivo* using *C. elegans*, they did not affect the growth and locomotion behavior of the worms. These results suggest that these peptides have a wider therapeutic window for treating H157 cancer cells. Theoretically, cancer cells possess more negatively charged components (e.g., phosphatidylserine and O-glycosylated mucins) on their surfaces compared to normal cells (Schweizer, 2009), and cationic AMPs are driven by electrostatic interactions, enabling them to interact with these components (Chiangjong et al., 2020). However, membrane permeabilization is not the sole mechanism by which AMPs exert antiproliferative effects on cancer cells. Long et al. demonstrated that dermaseptin PS1 inhibited the growth of U-251 MG cells by disrupting the cell membrane at high concentrations (10^{-5} M or higher), but induced apoptosis at a concentration of 10^{-6} M (Long et al., 2019). The reduced degree of α-helix and cationicity did not affect the antiproliferative activity of DPH1 and t-DPH1-NH_2 against H157 cells. This suggests that while C-terminal amidation plays an important role in antimicrobial activity, it does not appear to be necessary for antiproliferative activities. This hypothesis could be further tested by investigating the mechanism of action of these peptides on cancer cells.

5. Conclusions

In conclusion, the Trp^3 residue and the consensus motif of t-DPH1 play crucial roles in its bioactivities. The presence of a C-terminal amidation is not essential for the antiproliferative and antimicrobial activities of t-DPH1. The designed analogues t-DPH1-NH_2 retains significant potential for inhibiting the growth of human non-small lung cancer cells H157. Additionally, t-DPH1-NH_2 exhibits potent antimicrobial activity against Gram-negative bacteria, including *E. coli* and *K. pneumoniae*. Furthermore, t-DPH1-NH_2 demonstrates lower cytotoxicity and haemolytic activity, making it an ideal candidate for the development of potential antimicrobial and anticancer agents. This research provides the first systematic study on the effects of the three conserved features of the dermaseptin family on the bioactivities of dermaseptin peptides. The modification approach, starting with the conserved structure of a peptide family, offers new guidelines for reducing the toxicity of parent peptides and lays the foundation for further exploration of peptides within this family.

CRediT authorship contribution statement

Haixin Qin: Conceptualization, Methodology, Validation, Formal analysis, Investigation, Data curation, Writing – original draft, Writing – review & editing, Visualization. **Weimin Zuo:** Methodology, Validation, Formal analysis, Data curation, Visualization. **Siyuan Luo:** Methodology, Validation, Visualization. **Lilin Ge:** Software, Resources, Visualization. **Lei Wang:** Software, Visualization. **Xiaoling Chen:** Software, Visualization. **Chengbang Ma:** Software, Visualization. **Hong-Ye Li:** Resources, Writing – review & editing. **Tianbao Chen:** Conceptualization, Resources, Writing – review & editing, Supervision. **Mei Zhou:** Conceptualization, Validation, Formal analysis, Investigation, Data curation, Writing – original draft, Writing – review & editing, Supervision. **Hang Fai Kwok:** Conceptualization, Formal analysis, Resources, Writing – original draft, Writing – review & editing, Supervision, Project administration, Funding acquisition.

Declaration of competing interest

The authors declare that they have no known competing financial interests or personal relationships that could have appeared to influence the work reported in this paper.

Acknowledgement

This research was funded by the Science and Technology Development Fund of Macau SAR (FDCT) (file no. 0010/2021/AFJ), the Ministry of Education – Frontiers Science Center for Precision Oncology (MoE-FSCPO) University of Macau (UM) [file no. SP2023-00001-FSCPO], and the Faculty of Health Sciences (FHS) UM. H.Q. was in receipt of a postdoctoral fellowship from the FDCT. W.Z. and S.L. were in receipt of a PhD Assistantship from the FHS UM. The authors would like to thank the Proteomics, Metabolomics & Drug Development Core at FHS UM for advising on the circular dichroism experiment.

Appendix A. Supplementary material

Supplementary data to this article can be found online at https://doi.org/10.1016/j.arabjc.2023.105420.

References

Abed, M., Zoubi, K.A., Theurer, M., et al., 2013. Effect of dermaseptin on erythrocytes. Basic Clin. Pharmacol. Toxicol. 113, 347–352.
Amiche, M., Galanth, C., 2011. Dermaseptins as models for the elucidation of membrane-acting helical amphipathic antimicrobial peptides. Curr. Pharm. Biotechnol. 12, 1184–1193.

Arias, M., Nguyen, L.T., Kuczynski, A.M., et al., 2014. Position-dependent influence of the three Trp residues on the membrane activity of the antimicrobial peptide, tritrpticin. Antibiotics (Basel) 3, 595–616.
Bartels, E.J.H., Dekker, D., Amiche, M., 2019. Dermaseptins, multifunctional antimicrobial peptides: A review of their pharmacology, effectivity, mechanism of action, and possible future directions. Front. Pharmacol. 10, 1421.
Bradbury, A.F., Finnie, M.D., Smyth, D.G., 1982. Mechanism of C-terminal amide formation by pituitary enzymes. Nature 298, 686–688.
Brand, G.D., Leite, J.R., de Sa Mandel, S.M., et al., 2006. Novel dermaseptins from Phyllomedusa hypochondrialis (Amphibia). Biochem. Biophys. Res. Commun. 347, 739–746.
Brogden, K.A., 2005. Antimicrobial peptides: pore formers or metabolic inhibitors in bacteria? Nat. Rev. Microbiol. 3, 238–250.
Chakraborty, S., Rahman, T., 2012. The difficulties in cancer treatment. Ecancermedicalscience 6, ed16.
Chen, T., Luo, S., Wang, X., et al., 2021. Polyphenols from Blumea laciniata extended the lifespan and enhanced resistance to stress in caenorhabditis elegans via the insulin signaling pathway. Antioxidants (Basel) 10.
Chiangjong, W., Chutipongtanate, S., Hongeng, S., 2020. Anticancer peptide: Physicochemical property, functional aspect and trend in clinical application (Review). Int J Oncol 57, 678–696.
Conceicao, K., Konno, K., Richardson, M., et al., 2006. Isolation and biochemical characterization of peptides presenting antimicrobial activity from the skin of Phyllomedusa hypochondrialis. Peptides 27, 3092–3099.
Daum, J.M., Davis, L.R., Bigler, L., et al., 2012. Hybrid advantage in skin peptide immune defenses of water frogs (Pelophylax esculentus) at risk from emerging pathogens. Infect Genet Evol 12, 1854–1864.
David, H.E., Dawe, A.S., de Pomerai, D.I., et al., 2003. Construction and evaluation of a transgenic hsp16-GFP-lacZ Caenorhabditis elegans strain for environmental monitoring. Environ Toxicol Chem 22, 111–118.
Greber, K.E., Dawgul, M., 2017. Antimicrobial peptides under clinical trials. Curr Top Med Chem 17, 620–628.
He, H., Chen, Y., Ye, Z., et al., 2020. Modification and targeted design of N-terminal truncates derived from brevinin with improved therapeutic efficacy. Biology (Basel) 9.
Hu, W., Lee, K.C., Cross, T.A., 1993. Tryptophans in membrane proteins: indole ring orientations and functional implications in the gramicidin channel. Biochemistry 32, 7035–7047.
Huang, L., Chen, D., Wang, L., et al., 2017. Dermaseptin-PH: A novel peptide with antimicrobial and anticancer activities from the skin secretion of the south american orange-legged leaf frog, pithecopus (Phyllomedusa) hypochondrialis. Molecules 22.
Huang, Y., Huang, J., Chen, Y., 2010. Alpha-helical cationic antimicrobial peptides: relationships of structure and function. Protein Cell 1, 143–152.
Jenssen, H., Hamill, P., Hancock, R.E., 2006. Peptide antimicrobial agents. Clin. Microbiol. Rev. 19, 491–511.
Lee, D.G., Kim, H.N., Park, Y., et al., 2002. Design of novel analogue peptides with potent antibiotic activity based on the antimicrobial peptide, HP (2–20), derived from N-terminus of Helicobacter pylori ribosomal protein L1. Biochim. Biophys. Acta 1598, 185–194.
Lei, J., Sun, L., Huang, S., et al., 2019. The antimicrobial peptides and their potential clinical applications. Am. J. Transl. Res. 11, 3919–3931.
Li, B., Lyu, P., Xi, X., et al., 2018. Triggering of cancer cell cycle arrest by a novel scorpion venom-derived peptide-Gonearrestide. J. Cell Mol. Med. 22, 4460–4473.
Li, H., Zeng, L., Wang, C., et al., 2022. Review of the toxicity and potential molecular mechanisms of parental or successive exposure to environmental pollutants in the model organism Caenorhabditis elegans. Environ. Pollut. 311, 119927.
Liang, D., Li, H., Xu, X., et al., 2019. Design, screening and antimicrobial activity of novel peptides against Streptococcus mutans. Nan Fang Yi Ke Da Xue Xue Bao 39, 823–829.
Lin, T.A., Huang, C.W., Wei, C.C., 2022. Early-life perfluorooctanoic acid (PFOA) and perfluorooctane sulfonic acid (PFOS) exposure cause obesity by disrupting fatty acids metabolism and enhancing triglyceride synthesis in Caenorhabditis elegans. Aquat. Toxicol. 251, 106274.
Liu, S., Lin, Y., Liu, J., et al., 2022. Targeted modification and structure-activity study of GL-29, an analogue of the antimicrobial peptide palustrin-2ISb. Antibiotics (Basel) 11.
Long, Q., Li, L., Wang, H., et al., 2019. Novel peptide dermaseptin-PS1 exhibits anticancer activity via induction of intrinsic apoptosis signalling. J. Cell Mol. Med. 23, 1300–1312.
Lu, Y., Zou, W., Wang, L., et al., 2022. Kassporin-KS1: A novel pentadecapeptide from the skin secretion of Kassina senegalensis: Studies on the structure-activity relationships of site-specific "Glycine-Lysine" motif insertions. Antibiotics (Basel) 11.
Ma, R., Wong, S.W., Ge, L., et al., 2020. In vitro and MD simulation study to explore physicochemical parameters for antibacterial peptide to become potent anticancer peptide. Mol. Ther. Oncol. 16, 7–19.
Mechlia, M.B., Belaid, A., Castel, G., et al., 2019. Dermaseptins as potential antirabies compounds. Vaccine 37, 4694–4700.
Munita, J.M., Arias, C.A., 2016. Mechanisms of antibiotic resistance. Microbiol. Spectr. 4.
Mwangi, J., Hao, X., Lai, R., et al., 2019. Antimicrobial peptides: new hope in the war against multidrug resistance. Zool. Res. 40, 488–505.
Nguyen, L.T., Haney, E.F., Vogel, H.J., 2011. The expanding scope of antimicrobial peptide structures and their modes of action. Trends Biotechnol. 29, 464–472.
Nicolas, P., El Amri, C., 2009. The dermaseptin superfamily: a gene-based combinatorial library of antimicrobial peptides. Biochim. Biophys. Acta 1788, 1537–1550.
P. Norouzi, M. Mirmohammadi, and M. H. Houshdar Tehrani, Anticancer peptides mechanisms, simple and complex, Chem Biol Interact, (2022), 110194.
Ongey, E.L., Pflugmacher, S., Neubauer, P., 2018. Bioinspired designs, molecular premise and tools for evaluating the ecological importance of antimicrobial peptides. Pharmaceuticals (Basel) 11.
Oren, Z., Shai, Y., 1998. Mode of action of linear amphipathic alpha-helical antimicrobial peptides. Biopolymers 47, 451–463.
Qin, H., Fang, H., Chen, X., et al., 2021. Exploration of the structure-function relationships of a novel frog skin secretion-derived bioactive peptide, t-DPH1, through use of rational design, cationicity enhancement and in vitro studies. Antibiotics (Basel) 10.
Schweizer, F., 2009. Cationic amphiphilic peptides with cancer-selective toxicity. Eur. J. Pharmacol. 625, 190–194.
Sharma, K., Aaghaz, S., Shenmar, K., et al., 2018. Short antimicrobial peptides. Recent Pat. Antiinfect. Drug Discov. 13, 12–52.
Swain, S.C., Keusekotten, K., Baumeister, R., et al., 2004. C. elegans metallothioneins: new insights into the phenotypic effects of cadmium toxicosis. J. Mol. Biol. 341, 951–999.
Thompson, A.H., Bjourson, A.J., Orr, D.F., et al., 2007. A combined mass spectrometric and cDNA sequencing approach to the isolation and characterization of novel antimicrobial peptides from the skin secretions of Phyllomedusa hypochondrialis azurea. Peptides 28, 1331–1343.
Torres, M.D.T., Sothiselvam, S., Lu, T.K., et al., 2019. Peptide design principles for antimicrobial applications. J. Mol. Biol. 431, 3547–3567.
Van Epps, H.L., 2006. Rene Dubos: unearthing antibiotics. J. Exp. Med. 203, 259.
Vineeth Kumar, T.V., Sanil, G., 2017. A review of the mechanism of action of amphibian antimicrobial peptides focusing on peptide-membrane interaction and membrane curvature. Curr. Protein Pept. Sci. 18, 1263–1272.
Wu, D., Gao, Y., Tan, Y., et al., 2018. Discovery of distinctin-like-peptide-PH (DLP-PH) from the skin secretion of Phyllomedusa hypochondrialis, a prototype of a novel family of antimicrobial peptide. Front. Microbiol. 9, 541.
Xu, X., Lai, R., 2015. The chemistry and biological activities of peptides from amphibian skin secretions. Chem. Rev. 115, 1760–1846.
Yau, W.M., Wimley, W.C., Gawrisch, K., et al., 1998. The preference of tryptophan for membrane interfaces. Biochemistry 37, 14713–14718.
Ye, Z., Zhou, X., Xi, X., et al., 2022. In vitro & in vivo studies on identifying and designing temporin-1CEh from the skin secretion of Rana chensinensis as the optimised antibacterial prototype drug. Pharmaceutics 14.
Zairi, A., Tangy, F., Bouassida, K., et al., 2009. Dermaseptins and magainins: antimicrobial peptides from frogs' skin-new sources for a promising spermicides microbicides-a mini review. J. Biomed. Biotechnol. 2009, 452567.
Zhang, L., Wang, S., Zhao, Y., et al., 2022. Long-term exposure to polystyrene nanoparticles causes transgenerational toxicity by affecting the function and expression of MEV-1 and DAF-2 signals in Caenorhabditis elegans. NanoImpact 26, 100403.